A MODELING OF VORTEX RINGS IN AN AXISYMMETRIC PULSED JET

TADACHIKA SENO, SHIZUO KAGEYAMA AND RYUZO ITO
College of Engineering, Shizuoka University, Hamamatsu 432

Key Words: Fluid Mechanics, Axisymmetric Jet, Vortex Ring, Vortex Filament, Strouhal Number, Free Shear Layer, Biot-Savart's Law

The behavior of vortex rings in the initial region of an axisymmetric pulsed jet was simulated by replacing an annular shear layer with a particular vorticity distribution by an array of discrete vortex ring filaments. This modeling was restricted to an inviscid and axisymmetric condition. Consequently, the detailed structure in a real jet cannot be explained by this model. Nonetheless, it provided a good representation of the rolling-up of the shear layer, the vortex ring formation and the transport velocity of the vortex ring. The experimental result, that the pattern of vortex ring formation was roughly classified into three types by Strouhal number, was also explained by this model. The behavior of the vortex ring after formation (for example, vortex ring coalescence) was successfully simulated by replacing a vortex ring by a single vortex ring filament. It was found that vortex ring motion in the initial region of a jet was essentially inviscid.

Introduction

Mathematical models of inviscid vortex filaments have been frequently employed to explain phenomena in fluid mechanics, aerodynamics and meteorology. The availability of high-speed computers and recent experimental evidence of organized vortex-like structures in turbulent shear layers have stimulated the numerical modeling of flow fields by interacting vortices. The use of numerical techniques to study the motion of continuous vortex sheets represented by discrete arrays of point vortices is not new. The first work of significance in this field was that of Rosenhead,[6] who used a line of point vortices to represent a single vortex sheet in order to compute the effect of a sinusoidal perturbation on the motion of the sheet. The successful explanation of phenomena, that the shear layer rolled up and the vortex ring formed in an axisymmetric jet, was found by Michalke[4] by use of the linear stability theory. Streaklines in the rolling-up shear layer were calculated and compared with photographs of visualized axisymmetric unforced jets. Grant[3] reported that the flow field in the initial region of an axisymmetric jet was realized by numerical integration of the time-dependent Navier–Stokes equations. The calculaltion result showed that the flow field was dominated by the large-scale vortex ring structure observed experimentally. But this calculation required great amounts of computer storage and time.

In the present work, a simple numerical approach was used to study the rolling-up of a vortex sheet in an axisymmetric pulsed jet, replacing an annular shear layer with a particular vorticity distribution by an array of identical vortex ring elements. The effect of parameters (the pulsation amplitude, the smoothing distance, etc.) used in this numerical technique was investigated. The effect of Sr_0 on the jet behavior has been investigated experimentally by many authors.[2] However, numerical modeling of the flow field in the pulsed jet for a wide range of Sr_0 has not been reported. This modeling is expected to provide some interpretation of the features observed experimentally in pulsed jets for a wide range of Sr_0.

Received December 6, 1986. Correspondence concerning this article should be addressed to T. Seno.

1. Calculation Method

Two vortex ring elements, i, j were respectively located at x_i, x_j in cylindrical coordinates (x, r, ϕ) as shown in **Fig. 1**. The induced velocity of the point $\boldsymbol{P}(x_i, r_i, 0)$ on the vortex ring element i caused by the small volume dV in the vortex ring element j is expressed as Eq. (1) according to Biot–Savart's law.

$$\delta \boldsymbol{V}_{ij}=[(\boldsymbol{\omega}_j \times \boldsymbol{r}_0)/(4\pi r_0^3)]dV \tag{1}$$

where

$$dV=\sigma r_j d\phi\ , \quad r_0^2=(x_i-x_j)^2+r_i^2+r_j^2-2r_i r_j\cos\phi\ ,$$

and r_i, r_j denote the radii of the two vortex ring elements. σ and ω_j are the area of cross section of vortex ring filament j and the vorticity of dV respectively. Assuming that vortex ring elements i, j are axisymmetric, the total induced velocity of point $\boldsymbol{P}$ from the whole of vortex ring element j is expressed as

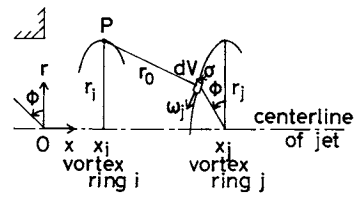

Fig. 1. Induced velocity between vortex ring filaments

Eq. (2).

$$V_{ij}=\int_V dV_{ij}=\frac{\sigma r_j}{4\pi r_0^3}\int_0^{2\pi}(\omega_j\times r_0)d\phi \qquad (2)$$

X component and r component of V_{ij} are expressed as follows:

$$V_{ijx}=\frac{\Gamma_j r_j}{2\pi r_0^3}\int_0^{\pi}(r_j-r_i\cos\phi)d\phi \qquad (3\text{-a})$$

$$V_{ijr}=-\frac{\Gamma_j r_j}{2\pi r_0^3}\int_0^{\pi}(x_j-x_i)\cos\phi d\phi \qquad (3\text{-b})$$

where

$$\Gamma_j=\omega_j\sigma\,,\qquad \omega_j=|\boldsymbol{\omega}_j|\,.$$

The self-induced velocity of vortex ring element i has only x component and is assumed as follows:

$$V_{si}/U_0=k(D/r)(\Gamma_i/\Gamma_0) \qquad (4)$$

where U_0 is the mean centerline velocity of the jet and D is the nozzle diameter. k is a proportional constant. The mean velocity at $r=D/2$ near the nozzle exit was about $0.7U_0$ in the experiments. On the assumption that vortex ring elements at $r=D/2$ near the nozzle exit were swept downstream by the speed of $0.7U_0$, k was set at 0.35 in this computation.

The process of the rolling-up of disturbed free shear layer and the vortex growth were described by the motion of each vortex ring element. The subsequent position of each ring element was calculated from the total velocity induced in each ring. This velocity was the sum of the self-induced velocity, Eq. (4), and the total induced velocity caused by all other vortex elements, computed from Eqs. (3-a, b). The new position of each vortex ring element was given approximately by:

$$\boldsymbol{P}_i(t+\Delta t)=\boldsymbol{P}_i(t)+\boldsymbol{V}_i(t)\Delta t+(d\boldsymbol{V}_i(t)/dt)(\Delta t)^2/2$$

Therefore

$$\boldsymbol{P}_i(t+\Delta t)=\boldsymbol{P}_i(t)+\{3\boldsymbol{V}_i(t)-\boldsymbol{V}_i(t-\Delta t)\}(\Delta t/2) \qquad (5)$$

where $\boldsymbol{P}_i$ is (x_i, r_i), the position of the ith vortex ring element, and $\boldsymbol{V}_i$ is the corresponding velocity.

The computation time was reduced further by neglecting the velocity field induced by any ring element beyond an axial distance D from the observational ring element. Calculations showed that the velocity ignored was less than 0.2% of the self-induced velocity of the vortex ring element. The effect of vortex ring elements beyond D, though cumulative, was small compared with the total velocity induced by closer vortex ring elements. The velocity induced by any vortex ring element beyond $D/2$, $3D/2$ or $2D$ was respectively less than 0.54%, 0.08% and 0.03% of the self-induced one.

The digitization of the shear layer caused small instabilities owing to high induced velocities by neighboring vortex ring elements. The "smoothing distance" was defined as a constant fraction of D. For $D/20$–$D/30$, the position of vortex ring formation as a cluster of vortex ring elements became far downstream from the nozzle exit because of the small induced velocity caused by other vortex ring elements. The calculation results were not coincident with the experimental ones. For $D/50$–$D/30$, small-scale instability was often observed for large values of Sr_0. As a result, the smoothing distance was set at $D/40$ in this computation. Induced velocities within the smoothing distance were obtained by linearly interpolating with the ratio of the distance between the two vortex ring elements to the smoothing distance.

A non-dimensional time parameter, T, was defined as $T=U_0t/D$. As a result of checking the effect of the time step for various values of Re and Sr_0, no effect of the time step on calculation results was observed for values of T less than 0.03. The time step, DT, was set at about 0.026 in this computation.

The strength of each vortex ring element, i.e., the circulation Γ, was determined by the strength of vortex sheet per unit length and the number of vortex ring elements per unit length, n. On the assumption that the velocity profile in the shear layer was not varying in the axial direction near the nozzle exit, the circulation along the four sides of a square which surrounded the shear layer was expressed as $U_0\times L$. L was the length of the square side in the jet core region. Consequently, the strength of the vortex sheet per unit length was adopted as U_0. The effect of pulsation was incorporated into the model by causing the vortex ring element circulation to fluctuate harmonically. The fluctuating strength of the ith vortex ring element was defined as:

$$\Gamma_i=\Gamma_0(1+A\sin 2\pi f_0t) \qquad (6)$$

where $\Gamma_0=U_0/n$. At the time the ith vortex ring element left the nozzle exit, the circulation, Γ_i, was fixed at that current value. Calculating Eq. (5) with Eqs. (3-a, b), (4) and (6), the motion of the continuous vortex sheet was represented by that of discrete vortex ring elements.

2. Result of Calculation and Discussion

The process of rolling-up of the shear layer is

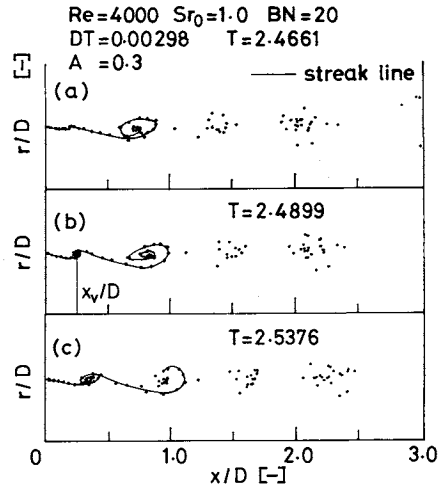

Fig. 2. Feature of rolling-up of shear layer

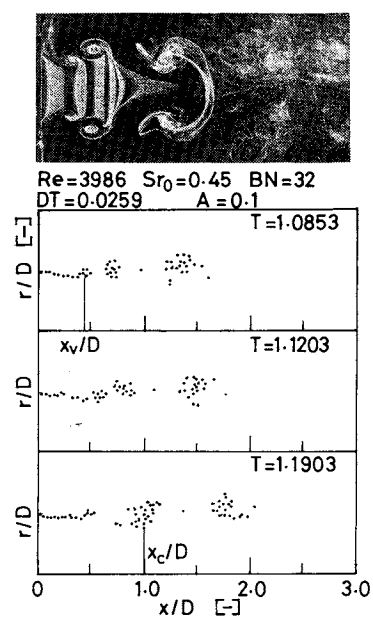

Fig. 3. Visualization of jet and feature of vortex ring formation in computation

described by motions of vortex ring elements for $Re=4000$, $Sr_0=1.0$, $A=0.3$ and $BN=20$ in **Fig. 2**. BN denotes the number of vortex ring elements per wave length of pulsation. "S shape" instability of array of vortex ring elements is observed at nearly $x/D=0.2$ in Fig. 2(a). Vortex ring formation as a cluster of vortex ring elements is observed at nearly $x/D=0.3$ in Fig. 2(b). The growth of the vortex ring by gathering nearby vortex ring elements is described in Fig. 2(c). The frequency of vortex ring formation was coincident with that of pulsation. This model, in which an annular shear layer was replaced by an array of identical vortex ring elements, provided a good interpretation of vortex ring formation experimentally observed in a real jet.

Computations were done for $Re=2000$, 4000 and 6000 with various Sr_0 values in the range of 0.3–5.2. It was found that the pattern of vortex ring formation in

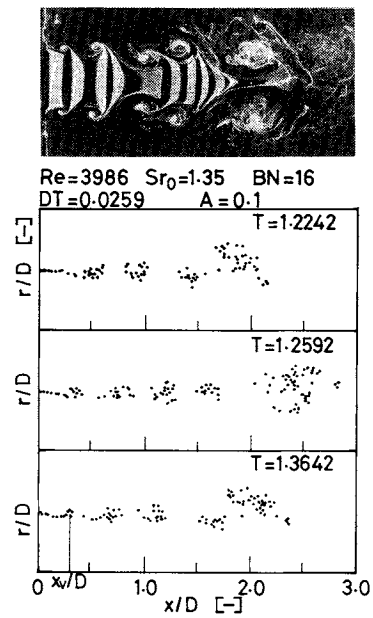

Fig. 4. Visualization of jet and feature of vortex ring formation in computation

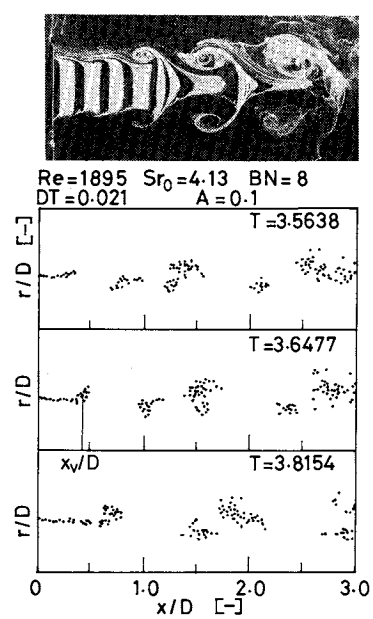

Fig. 5. Visualization of jet and feature of vortex ring formation in computation

the computation was roughly classified into three types by Sr_0. For $0.3<Sr_0<0.9$, one pair of vortex rings, a larger one and a smaller one, was produced at the same periodic intervals as the pulsation. The result of calculation and the visualization of the real jet for $Re=3986$, $Sr_0=0.45$ are shown in **Fig. 3**. The vortex ring (shown in the photograph) is represented as a cluster of vortex ring elements (shown as a cluster of points in the figures) in this calculation. For $0.9\leqq Sr_0\leqq 2.0$, equal-sized vortex rings were produced distinctly at the same periodic intervals as the pulsation (cf. **Fig. 4**). For $2.6<Sr_0$, vortex rings were produced independently of Sr_0 (cf. **Fig. 5**). This result

of calculations was coincident with the experimental result reported in the previous paper.[7] However, it was difficult to distinguish the vortex ring formation from small-scale instability, i.e., small groups of vortex ring elements, for the range of $2.0 < Sr_0 \leqq 2.6$. For $Sr_0 > 2.0$, small-scale instability was often observed because of the narrow space and the large difference in circulation between neighboring vortex ring elements. The position of vortex ring formation in the computation is compared with the experimental one in **Fig. 6**. The mean transport velocity of the vortex ring in the range of $0.5 < x/D < 2.5$ is shown in **Fig. 7**. The calculated data were coincident with the experimental data of Petersen,[5] but were slightly lower than our experimental data. This simulation seems to be a good representation of a pulsed jet observed experimentally as concerns the position of vortex ring formation and the transport velocity of the vortex ring. The position of vortex ring coalescence, x_c, is related to Sr (based on passage frequency of vortex ring) as shown in **Fig. 8**. For $0.5 < Sr < 2.0$, the correlation $x_c/D = 1.2Sr^{-1}$ was obtained in our experiments while Petersen proposed the experimental correlation $x_c/D = Sr^{-1}$. For that range of Sr, calculated data showed a trend similar to that of the two correlations, though data were rather scattered. For $2.0 < Sr < 2.6$, the calculated data were rather larger than experimental ones and were unreliable because of small-scale instability. This simulation was not a good representation of the vortex ring coalescence observed experimentally. The circulation is an important factor in simulating the process of coalescence. The scattering of data appeared to be caused by an unreasonable evaluation of the circulation. It appeared doubtful that the circulation of the vortex ring in coalescing was the sum of circulations of vortex ring elements which represented the shear layer. So the vortex ring behavior after formation was simulated by replacing a vortex ring by a single vortex ring element, not by a cluster of vortex ring elements, assuming that circulation of vortex ring elements which concern the coalescence could be evaluated by Eq. (3-b) with use of r directional displacements of the two vortex ring elements. An example of the calculation result is shown in **Fig. 9**. Trajectories of the two vortex rings which concern the coalescence are coincident with calculated ones except in the region where the two vortex rings are close together.

In this way, vortex ring behavior in the initial region of an axisymmetric jet was simulated by the inviscid model according to Biot-Savart's law. Acton[1] also concluded that the large eddy motion in this region was essentially inviscid.

The effect of the pulsation amplitude was investigated by varying the value of A from 0.005 to 0.3 for various Re and Sr_0. When A was larger than 0.05,

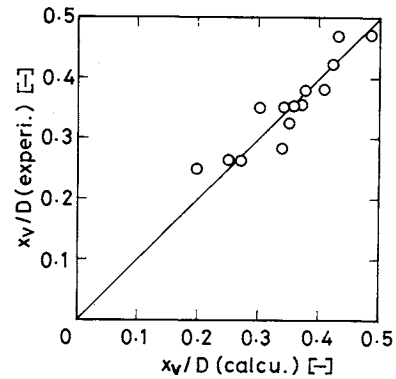

Fig. 6. Position of vortex ring formation

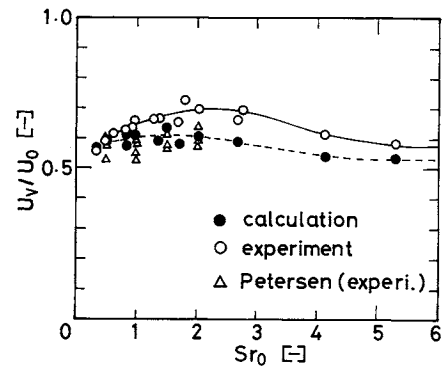

Fig. 7. Transport velocity of vortex ring

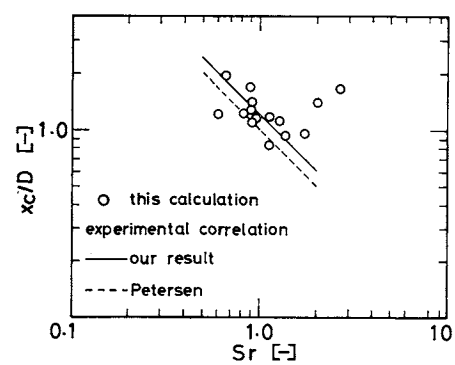

Fig. 8. Position of vortex ring coalescence

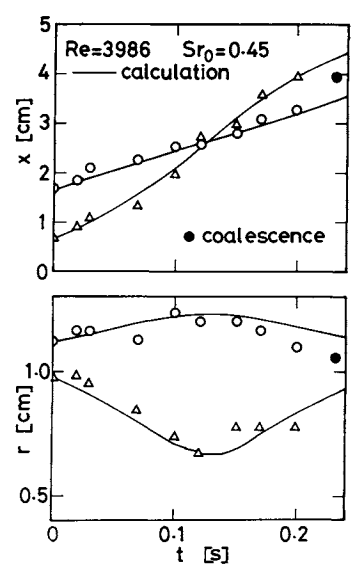

Fig. 9. Trajectories of vortex rings in coalescing

the effect of pulsation was observed. With an increase of A over 0.05, clearer distinct vortex rings were produced, and a small effect of A on the position of vortex ring formation was observed. No effect of A on the pattern of vortex ring formation was observed.

Conclusion

This simulation, in which an annular shear layer (or vortex sheet) was replaced by an array of discrete vortex ring elements, provided a good representation of the rolling-up of the shear layer in the axisymmetric pulsed jet. The experimental result, that the pattern of vortex ring formation was roughly classified into three types by Sr_0 was successfully explained by this simulation. The simulation was also a good representation of vortex ring behavior observed experimentally as concerns the position of vortex ring formation and the transport velocity of the vortex ring. The behavior of the vortex ring after formation (for example, vortex ring coalescence) was successfully simulated by replacing a vortex ring by a single vortex ring filament. It was found that vortex ring motion in the initial region of a jet was essentially inviscid.

Nomenclature

A	=	amplitude of pulsation	[—]
BN	=	number of vortex ring elements per wave length of pulsation	[—]
D	=	nozzle diameter	[m]
DT	=	dimensionless time step	[—]
f	=	mean passage frequency of vortex ring	[Hz]
f_0	=	frequency of pulsation	[Hz]
k	=	a proportional constant	[—]
n	=	number of vortex ring elements per unit length	[—]
Re	=	$\rho DU_0/\mu$, Reynolds number	[—]
Sr	=	fD/U_0, Strouhal number	[—]
Sr_0	=	f_0D/U_0, Strouhal number	[—]
T	=	U_0t/D, dimensionless time	[—]
t	=	time	[s]
U_0	=	mean centerline velocity of jet	[m s^{-1}]
$\boldsymbol{V}$	=	induced velocity vector	[m s^{-1}]
V_s	=	self-induced velocity	[m s^{-1}]
x_c	=	x position of vortex ring coalescence	[m]
x_v	=	x position of vortex ring formation	[m]
Γ	=	circulation of vortex	[m^2 s^{-1}]
μ	=	viscosity of fluid	[Pa s]
ρ	=	density of fluid	[kg m^{-3}]
σ	=	area of cross section of ring filament	[m^2]
ω	=	vorticity vector	[s^{-1}]

〈Subscript〉

i,j	=	vortex ring element i, j

Literature Cited

1) Acton, E: *J. Fluid Mech.*, **98**, 1 (1980).
2) Crow, S. C. and F. H. Champagne: *J. Fluid Mech.*, **48**, 547 (1971).
3) Grant, A. J.: *J. Fluid Mech.*, **66**, 707 (1974).
4) Michalke, A.: *Zur Instabilität einer gestörten Scherschicht, Ingenieur-Archiv.*, **XXXIII**, 264 (1964).
5) Petersen, R. A.: *J. Fluid Mech.*, **89**, 469 (1978).
6) Rosenhead, L.: *Proc. Roy. Soc. A*, **134**, 170 (1931).
7) Seno, T., S. Kageyama and R. Ito: *J. Chem. Eng. Japan*, **20**, 128 (1987).